Available online at www.sciencedirect.com

ScienceDirect

Procedia CIRP 114 (2022) 94–99

www.elsevier.com/locate/procedia

17th CIRP Conference on Computer Aided Tolerancing

Repeatability of Dimensional Accuracy and Mechanical Properties in Powder Bed Fusion of 16MnCr5 using a Laser Beam

Matthias Schmitt[a]*, Georg Schlick[a], Joahnnes Schilp[a,b]

[a]Fraunhofer-Institute for Casting, Composite and Processing Technology IGCV, Am Technologiezentrum 10, 86159 Augsburg, Germany
[b]University of Augsburg, Chair of Digital Manufacturing, Department of Applied Computer Science, Universitaetsstraße 2, 86159 Augsburg, Germany

* Corresponding author. Phone: +49 821 90 678 147. Fax: +49 821 90 678 199. Email address: matthias.schmitt@igcv.fraunhofer.de

Abstract

Additive manufacturing, especially powder bed fusion using a laser beam of metals (PB-LB/M), allows the build-up of complex parts. Therefore, PBF-LB/M is already used in multiple fields, such as medical or aerospace industry. To promote the use of AM within the automotive sector materials such as case-hardening steels have been developed for PBF-LB/M to manufacture drivetrain parts e.g. gears. However, the automotive industry requires strict tolerances and repeatability in the manufacturing processes.
At first, the repeatability of specimens built with the case-hardening steel 16MnCr5 within one build plate is investigated. Therefore, the dimensional accuracy in x-, y- and z-direction is measured and ISO basic tolerances are derived. Additionally, the density of specimens within one build plate is determined. Both results are linked to the recoating direction and the occurring gas flow. In a second step, the repeatability between subsequent build jobs is analyzed. The tensile strength of specimens manufactured in 12 build jobs of similar layout is investigated showing high repeatability with properties exceeding conventional material. The occurring tolerances of more than 80 Type 1 gears in 20 build jobs are aggregated to evaluate the process capability of the PBF-LB/M process.

Keywords: Additive Manufacturing, PBF-LB/M, 16MnCr5, repeatability, dimensional accuracy, mechanical properties

1. Introduction

Additive manufacturing technologies are characterized by a build-up in layers, which gives great freedom in part designs that include lightweight structures (e.g. lattice) or integrated cooling channels [1]. With the given opportunities, new part designs and business models are evolving that include spare part supply and individualization [2]. Powder Bed Fusion with a Laser Beam of Metals (PBF-LB/M) is an additive manufacturing technology whereby metal alloy powder is melted by a laser beam in subsequent layers, with the possibility of reaching high part density [3]. At first, a layer of powder is recoated with typical layer heights from 20 to 120 µm. After this step the 2D dimensions of the part in this layer are solidified with a laser beam. Usually, the solidification consists of an infill of the part and a border exposure, which determines the dimension. At last, the baseplate is lowered before recoating takes place again [4]. The manufacturing steps in PBF-LB/M are depicted in Figure 1.

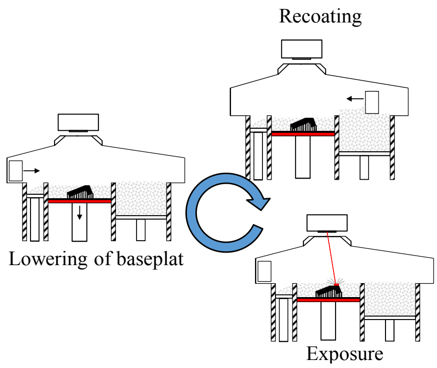

Figure 1 Process sequence of PBF-LB/M with the steps of recoating, exposure and baseplate lowering.

10.1016/j.procir.2022.10.013

Nomenclature and nominal gear dimensions

D_T	Tip diameter of the lightweight gear
D_B	Bore diameter of the lightweight gear
K_G	Key feather groove width of the lightweight gear
TF_W	Tooth flank width of the lightweight gear

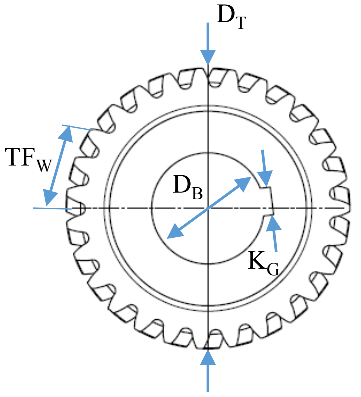

D_T:	101.00 mm	D_B:	39.60 mm
K_G:	10.00 mm	TF_W:	35.70 mm

PBF-LB/M allows the processing of corrosion resistant or tool steels, nickel base alloys, titanium alloys and aluminum alloys [5]. Case-hardening steel is materials group used for highly loaded drivetrain parts in the automotive industry e.g. gears and shift forks. The use in additive manufacturing has only recently become focus of research, mainly due to their higher carbon content of around 0.15 to 0.23 weight-% [6]. To establish PBF-LB/M in supply chains, to apply suitable machining allowances for functional surface and to design components, knowledge of the achievable accuracy and the repeatability of these and the mechanical properties are necessary.

Minetola et al. compared the dimensional accuracy of PBF-LB/M and PBF-EB/M (EB: electron beam) in a study with single standardized test artefact reporting ISO tolerance grades of IT 12 and 13 respectively according to ISO 286-1 [7]. When investigating the dimensional accuracy of a tooling component (30x30x27.2 mm³) manufactured by PBF-LB/M with AlSi10Mg over three consecutive build jobs no correlation between the deviation and the build plate position was seen [8]. Studying down facing surfaces in PBF-LB/M parts lead to the conclusion that the dross formation and spatter increase the occurring deviation and that the statistical nature of these phenomes complicate the prediction increasing the required machining allowance [9]. Peixin et al. showed that the part deviation strongly depends on the used material since deviation from an identical geometry doubled from 316L to IN718 highlighting the importance of thermal gradients [10].

In a review by Dowling et al. the repeatability of PBF-LB/M is identified as an underdeveloped research topic and hindrance for the industrial adoption stating a low "overall equipment effectiveness" (OEE) of only 30% [11]. Repeatable build jobs are mainly studied to investigate the recycling behavior of powders used in PBF-LB/M [12, 13]. Tang et al. showed that the tensile strength increases when reusing Ti6Al4V in PBF-EB/M more than 20 times due to the oxygen pick-up [14].

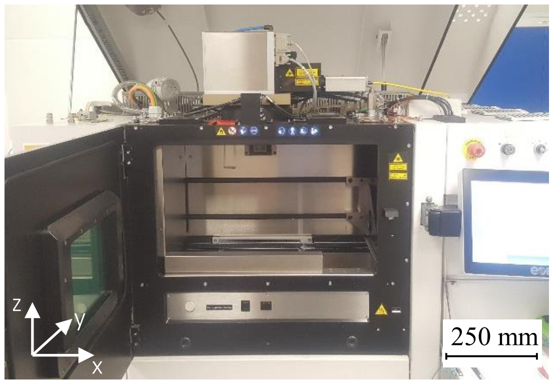

Figure 2 PBF-LB/M machine (EOS M290 from EOS GmbH, Germany) used for the study

Investigating the repeatability of 6 build jobs at varied packing density lead to the conclusion that the packing density has a significant effect on the mechanical properties while no correlation to the job number was found [15]. A detailed study investigated the tensile property distribution on the build plate showing that lower tensile strength can be seen if spatter is not sufficiently removed at certain build plate locations [16].

In conclusion, it becomes clear that there is currently a gap of knowledge in regard to the dimensional accuracy and repeatability of PBF-LB/M. The focus of this contribution is the investigation of the dimensional accuracy and part properties within the build plate and the repeatability between build jobs with simple specimens at first but then is followed with gears as a use case mimicking a small scale production.

1.1. Materials and methods

To manufacture the specimens, an EOS M 290 (EOS GmbH, Germany) machine was used applying a baseplate preheating of 80 °C and argon as shielding gas. Recoating took place with a carbon brush to minimize the risk of process interruptions. A layer thickness of 30 µm was chosen and the specimens were built with laser parameters derived from [17]. The machine is depicted in Figure 2. Particle size distribution was analyzed by laser diffraction with a Mastersizer 3000. The density was measured with the Archimedes principle using a fine scale with a precision of 0.001 g. Relative density values are mean values of three measurements and specimens. Tensile tests were carried out using a Zwick Roell Z050 according to DIN EN ISO 6892-1 with at least three specimens per build job (c.f. Fig. 3).

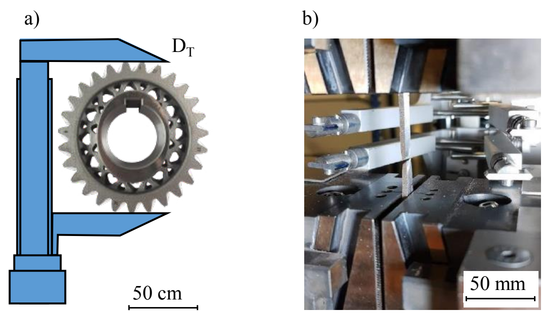

Figure 3 a) Schematic caliper measurement of the nominal top diameter (DT) b) Tensile testing set-up

Deviation from the target dimension was defined as the resulting value from subtracting the measured dimension from the CAD target dimensions. Measurements were taken with a digital caliper from Mitutoyo Corporation (Japan) with a MPE (maximum permissible error) of 20 µm according to ISO 10360.

To determine the dimensional accuracy on the build plate 621 cubes with the dimensions of 5x5x7 mm³ were built in an even arrangement (c.f. Figure 4). The density measurements represent the mean value of all specimens in an area of 50x50 mm² of the build plate. Additionally, the deviation occurring in large parts was calculated from lightweight gears

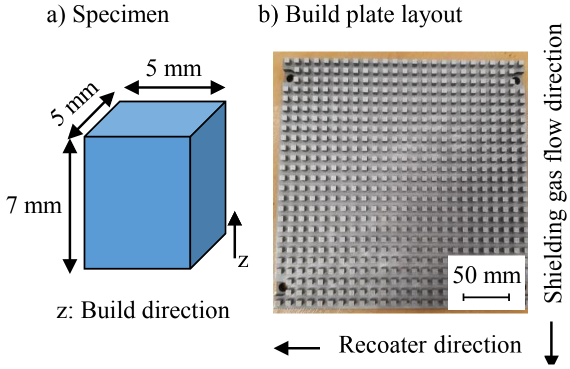

Figure 4 a) Dimension accuracy specimen b) layout of the build plate with 261 specimens

dimensions. The gears possess a nominal tip diameter of 101.00 mm, a nominal bore diameter of 39.60 mm, a nominal tooth flank width (4 teeth) of 35.70 mm and a nominal key feather groove width of 10.00 mm including manufacturing allowance for a hard finishing after case-hardening. All measurements on gears took place after they were removed from the build plate in succession to a residual stress relief annealing of the parts on the build plate at 600 °C for 5 h under argon atmosphere. The tensile specimen were in the same condition as they were built as process samples on the same build plate as the gears as shown in Figure 5. All specimens and gears were manufactured from the chase-hardening steel 16MnCr5 which is commonly used in gear manufacturing [18].

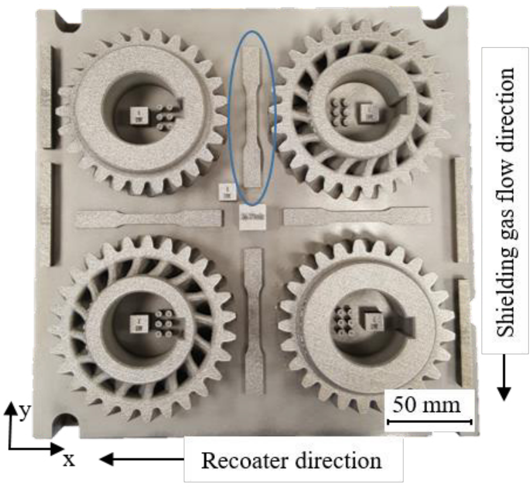

Figure 5 Build plate layout with 4 gears (2 lightweight gears, 2 conventional gears) including various process samples with flat tensile specimens (marked)

1.2 Case-hardening steel 16MnCr5

16MnCr5 (1.7131) is a low alloyed steel with case-hardening capabilities, and is increasingly used in PBF-LB/M [19]. The chemical composition of the powder is shown in Table 1. Particle size distribution is of approximately normal distribution, with a D10 of 28 µm, D50 of 47 µm and D90 of 72 µm. The powder is recycled during the manufacturing campaign and is sieved after every build job with a mesh size of 63 µm to remove spatter.

Table 1 Chemical composition of 16MnCr5 in % by mass 1) DIN EN10084 2) supplier certificate

	C	Mn	Cr	Si	P	S	Fe
1)	0.14-0.19	1.0-1.3	0.8-1.1	≤ 0.4	≤ 0.025	≤ 0.035	bal.
2)	0.15	1.05	0.9	0.19	-	-	bal.

2. Dimensional accuracy and density distribution within a build plate

Firstly, the described cubical specimens were built on one build plate with a distance of 5 mm from each other. Four specimen could not be manufactured due to the screws positioned at the corner of the plate. All specimens were measured with a caliper (5 measurements in each direction, mean values of three build jobs are represented) and the resulting deviation from the target CAD dimensions were calculated. The comparably small samples allow the detailed representation of the accuracy distribution over the build plate. The resulting deviation in x-, y-, and z-direction is shown in Figure 6.

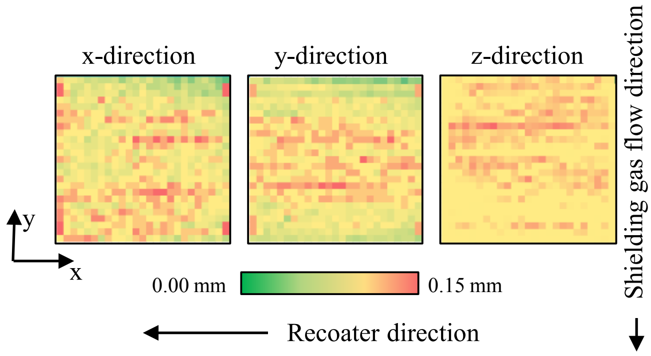

Figure 6 Deviation from CAD geometry in dependency of baseplate position

The deviation in x-direction lies mainly in a range from 0 to 0.05 mm. The opposite side to the shielding gas flow shows an increased deviation of 0.05 to 0.1 mm. No clear correlation is seen in the recoater direction. The deviation in y-direction is evenly distributed but shows increased deviation of 0.05 to 0.1 mm at the edges. The deviation in z-direction is higher compared to the x- or y-direction and a connection with the shielding gas flow can be seen leading to the highest deviations of 0.1 to 0.15 mm. In a next step, the ISO tolerance grades according to ISO 286-1 are calculated with the mean deviation of all cubes to get an overall view. In total it shows that IT tolerances grades of 12 are reached in x- and y-direction whereas the deviation in z-direction lies in IT tolerance grade 15 for the small cubic specimens (c.f. Table 2).

Table 2 Overall IT tolerance grades for the cubic specimens

	x-direction	y-direction	z-direction
ISO tolerance grade	12	12	15

Secondly, the dimensions of lightweight gears manufactured as depicted in Figure 5 were measured to gain insight into the dimensional accuracy of larger parts. All gears were measured with a caliper (5 measurements for each geometric feature, mean values of three build jobs are represented) and the resulting deviation from the target CAD dimension were calculated. The resulting deviations show no clear correlation with the position on the build plate as depicted in Figure 7. The key feather groove (K_G), the tip diameter (D_T) and the bore diameter (D_B) are undersized whereas the tooth flank width (TF_W) is increased compared to the CAD geometry data.

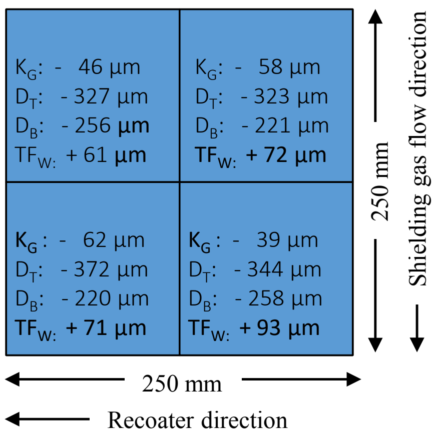

Figure 7 Deviation from CAD geometry of gears in dependency of the baseplate position

In a next step, the ISO tolerance grades according to ISO 286-1 are calculated for these larger components. The ISO tolerance grades range from 11 to 13 and are listed in Table 3.

Table 3 IT tolerance grades for specific geometric features of the gears

	K_G	D_T	D_B	TF_W
ISO tolerance grade	12	13	13	11

After investigating the dimensional accuracy of cubic specimens and lightweight gear components, the relative part density in regards to the build plate position were measured. The relative density is used as a performance indicator for the mechanical properties and is commonly used in quality determination in parts manufactured by PBF-LB/M [20]. All specimens were measured with the principle of Archimedes (3 measurements of each specimen, mean values of three build jobs are represented and all specimen in the 50x50 mm² build plate area are aggregated). The evaluation is shown in Figure 8 displaying a high correlation of the relative density and the

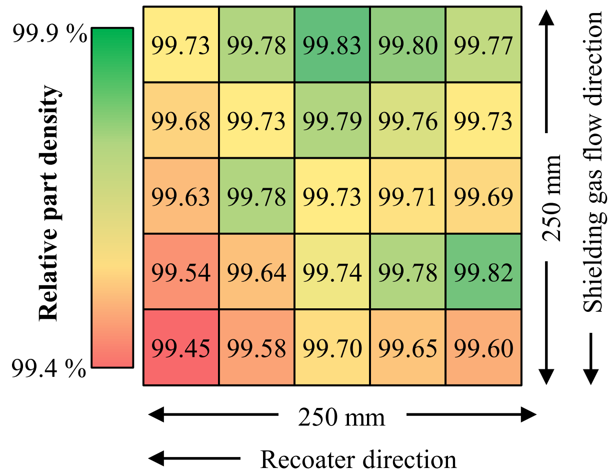

Figure 8 Relative density in dependency of the build plate position

build plate position. Lowest relative density is observed at the opposite side to the shielding gas flow and in the corner in recoater direction. The threshold of a relative density of 99.5 % by VDI 3405 (sheet 2) is not reached in this area and lower mechanical properties can be expected.

3. Repeatability of dimensional accuracy and tensile strength

Subsequently after determining the accuracy of parts and the dependency of the build plate position, the repeatability of the accuracy and the mechanical properties is studied. In a small scale production scenario 21 build jobs of four gears in an identical layout (c.f. Figure 5) were carried out leading to a total number of 84 gears. For each gear the bore diameter (D_B) and the tip circle diameter (D_T) were measured after the gears were removed from the build plate in succession to a residual stress relief annealing. The measurements were used to calculate the deviation from the CAD geometry data and are depicted in Figure 9. The data from the tip circle diameter can be aggregated in three cluster from gear 1-22, gear 22-45 and the

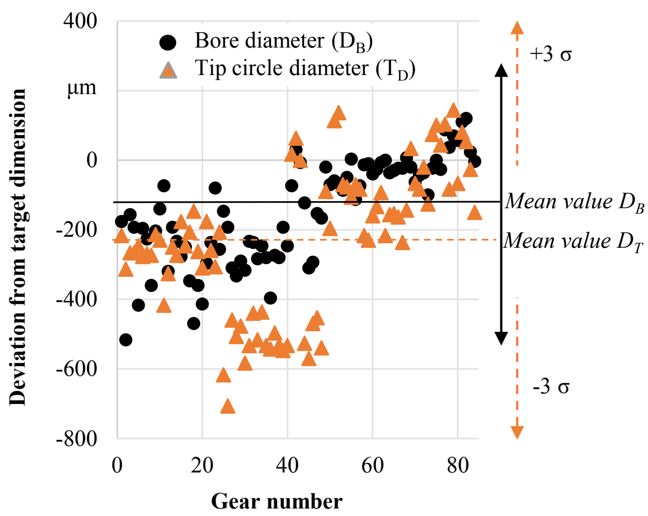

Figure 9 Repeatability of the dimensional accuracy

remaining gears. The gears from cluster 2 show the highest deviation in negative direction. All other gears show a lower deviation of the tip circle diameter. The presented data from the bore diameter deviation show a slight trend leading from -200 to +100 µm deviation. Consequently, the 6-sigma intervals are comparably large e.g. with more than 1 mm for the tip circle diameter.

Parallel to the measurements geometric measurements, the tensile samples form the first 12 build jobs were tested. Flat tensile specimens with a width of 2 mm were used as described in Section 1.1. The tests were conducted in the state after stress relief annealing which reduces the tensile strength by around 20 % compared to the as-built state [6]. The resulting tensile strength in dependency to the build job number is presented in Figure 10. A mean value of 820 N/mm² is reached exceeding the reference of 620 N/mm² of 16MnCr5 from conventional manufacturing (solution annealed). Minimal recorded values still surpass this threshold. In a closer observation, certain clusters of 4 tensile specimens from one build job can be identified with very similar values often distinctively higher or lower (around 75 N/mm²) than previous builds. In total, the repeatability of the mechanical properties show that the reference values are reached under all conditions in a small scale production scenario.

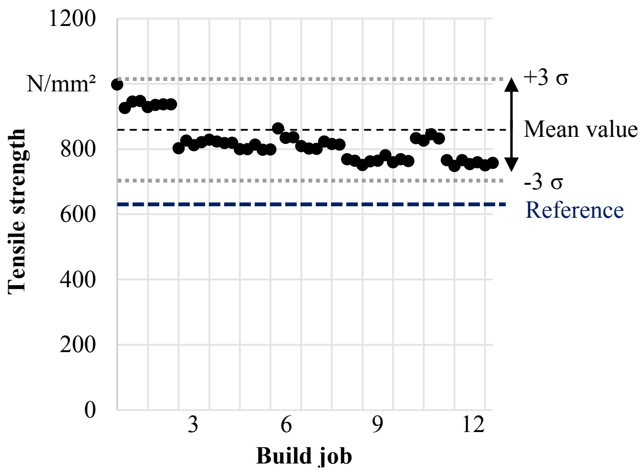

Figure 10 Repeatability of the tensile strength accuracy

4. Discussion

The dimensional accuracy of small parts shows a distribution on the build plate. In general, the opposite build plate side to the shielding gas flow and the edge areas of the build plate show higher deviations. During the process spatter occurs and is transported by the shielding gas flow. Insufficient shielding gas flow can lead to a spatter deposit on parts and in the powder bed. As the spatter particles are often lager than the powder particles the present local particle size distribution coarsens which can lead to an increase of the surface roughness [21]. The increased surface roughness then leads to an increased part size during the measurements. In combination with the comparably small specimen dimensions of 5x5x7 mm³ a high deviation and IT tolerance grades are calculated. With increased part size the effect of the increased surface roughness should be less dominant as seen when examining the deviations of the lightweight gears on the build plate. Here, no significant dependency on the part position can be seen. The occurring spatter formation and deposition on parts leads to issues during the solidification step as they cannot be molten as normal powder particles leading to material defects [15, 22]. With this in mind, the relative density distribution is mainly induced by spatter and highlights areas with insufficient shielding gas flow.

In terms of repeatability two distinctions need to be made. The repeatability of the mechanical properties in a tensile test show high reproducibility with a mean value of 820 N/mm² exceeding the reference threshold of 620 N/mm². The appearing coupled aggregation of 4 values could be an effect of slightly different stress relief annealing processes which were carried out on the baseplate after the PBF-LB/M process. Varied holding or cooling times or deviation of the temperature prevent the complete stress relief annealing or change the microstructure [6]. The build plates were gathered in groups of one to four plates for the stress relief annealing during the trials. This results in the regular group wise distribution of the tensile specimens through slightly different temperatures and cooling times. Therefore, it can be seen that the effect of the heat treatment is higher than effects from the AM process itself.

The reproducibility of the dimensional accuracy of the gears show a high deviation and no predictable pattern leading to high 6-sigma values. On the one hand, the distortion of the gears could lead to the conclusion that the stress relief annealing is not sufficient to mitigate the distortion. On the other hand, the deviation is not evenly distributed which could be influenced by the lightweight structure itself as it increases distortion which is also seen in conventional approaches for lightweight gears [23].Additionally, the used manual measurement with a caliper is operator dependent which has a part in the overall deviation. The decreased bore size leads to additional machining time during the bore grinding process. The decreased tip circle diameter requires a process adjustment during the flank grinding process. The low repeatability leads to increased set-up time during machining. In total, the high deviation and low repeatability lead to increased post-processing costs for the PBF-LB/M gears.

5. Summary and outlook

This paper presents an investigation of the dimensional accuracy and mechanical properties in PBF-LB/M with regard to the build plate location and the repeatability in a small scale production scenario. Small parts show a significant dependency of the occurring deviation to the build plate location and reach ISO tolerance grades from 12 to 15. Large parts show no correlation to the location and ISO tolerances are in the range of 11 to 13. The tensile properties show a high repeatability compared to the dimensional accuracy. Some effects can be attributed to insufficient shielding gas flow. The overall process chain including the stress relief annealing contributes to the repeatability of the mechanical properties but especially to the dimension accuracy due to part distortion.

The result of this study can be applied in industry for a small scale production to plan the process chain, especially the required machining steps in regard to the achievable IT tolerance grades. As an outlook, further in depth studies of the gear distortion using 3D optical scanners should be conducted for more insights. Additionally, the load carrying capacities of gears manufactured by PBF-LB/M from 16MnCr5 should be studied to establish the technology in the industry.

Acknowledgements

We extend our sincere thanks to the German Research Foundation (DFG) for providing the financial means for this research within the project RE1112-50/1 “Integrational lightweight design for gears by laser beam melting”.

References

[1] Thompson, M.K., Moroni, G., Vaneker, T., Fadel, G. et al., 2016. Design for Additive Manufacturing: Trends, opportunities, considerations, and constraints 65, p. 737.

[2] Lutter-Guenther, M., Seidel, S., Kamps, T., Reinhart, G., 2015. Implementation of Additive Manufacturing Business Models, p. 547.

[3] DIN-EN-ISO-ASTM-52900-2017-061.

[4] Gebhardt, A., 2016. Additive Fertigungsverfahren: Additive Manufacturing und 3D-Drucken fuer Prototyping - Tooling - Produktion, 5th edn. Hanser, Muenchen.

[5] Herzog, D., Seyda, V., Wycisk, E., Emmelmann, C., 2016. Additive manufacturing of metals 117, p. 371.

[6] Schmitt, M., Kamps, T., Siglmueller, F., Winkler, J. et al., 2020. Laser-based powder bed fusion of 16MnCr5 and resulting material properties 35, p. 101372.

[7] Paolo Minetola, Manuela Galati, Flaviana Calignano, Luca Iuliano, Giovanni Rizza, Luca Fontana, 2019. Comparison of dimensional tolerance grades for metal AM processes, p. 399.

[8] Zongo, F., Tahan, A., Aidibe, A., Brailovski, V., 2018. Intra- and Inter-Repeatability of Profile Deviations of an AlSi10Mg Tooling Component Manufactured by Laser Powder Bed Fusion 2, p. 56.

[9] Calignano, F., Iuliano, L., Galati, M., Minetola, P. et al., 2020. Accuracy of down-facing surfaces in complex internal channels produced by laser powder bed fusion (L-PBF) 88, p. 423.

[10] He, P., Sun, C., Wang, Y., 2021. Material distortion in laser-based additive manufacturing of fuel cell component: Three-dimensional numerical analysis 46, p. 102188.

[11] Dowling, L., Kennedy, J., O'Shaughnessy, S., Trimble, D., 2020. A review of critical repeatability and reproducibility issues in powder bed fusion 186, p. 108346.

[12] Ardila, L.C., Garciandia, F., González-Díaz, J.B., Álvarez, P. et al., 2014. Effect of IN718 Recycled Powder Reuse on Properties of Parts Manufactured by Means of Selective Laser Melting 56, p. 99.

[13] Keith Murray, Martin A. Kearns and Paul A Davies, 2017. The Influence of Powder Ageing Characteristics on 316L Stainless Steel processed by Laser based Powder Bed Fusion.

[14] Tang, H.P., Qian, M., Liu, N., Zhang, X.Z. et al., 2015. Effect of Powder Reuse Times on Additive Manufacturing of Ti-6Al-4V by Selective Electron Beam Melting 67, p. 555.

[15] Haeckel, F., Meixlsperger, M., Burkert, T., 2017. Technological challenges for automotive series production in laser beam melting Solid Freeform Fabrication 2017: Proceedings of the 28th Annual International.

[16] Haeckel, F., 2020. Reproduzierbarkeit des Laserstrahlschmelzens im Hinblick auf einen Einsatz in der automobilen Serienproduktion, Aachen.

[17] Schmitt, M., Schlick, G., Seidel, C., Reinhart, G., 2018. Examination of the Processability of 16MnCr5 by Means of Laser Powder Bed Fusion.

[18] Niemann, G., Winter, H., 2003. Maschinenelemente: Band 2: Getriebe allgemein, Zahnradgetriebe - Grundlagen, Stirnradgetriebe. Springer Berlin Heidelberg, Berlin, Heidelberg,

[19] Clare, A.T., Mishra, R.S., Merklein, M., Tan, H. et al., 2022. Alloy design and adaptation for additive manufacture 299, p. 117358.

[20] VDI, 2014. VDI-Richtlinie 3405 Blatt 2: Strahlschmelzen metallischer Bauteile - Qualifizierung, Qualitaetssicherung und Nachbearbeitung.

[21] Lutter-Guenther, M., Broeker, M., Mayer, T., Lizak, S. et al., 2018. Spatter formation during laser beam melting of AlSi10Mg and effects on powder quality 74, p. 33.

[22] Ladewig, A., Schlick, G., Fisser, M., Schulze, V. et al., 2016. Influence of the shielding gas flow on the removal of process by-products in the selective laser melting process 10, p. 1.

[23] Luebben, T., Surm, H., Hoffmann, F., Zoch, H.-W., 2016. Identification of design related distortion of gear base bodies by experimental investigations 47, p. 678.